Seismic Response and Retrofit Design Recomendations for Braced Steel Bridge Piers

By Jeffrey W. Berman[1] and Michel Bruneau[2]

ABSTRACT

Braced piers of steel truss bridges having braces with latticed built-up cross-sections may suffer significant damage during earthquakes due to the buckling, rapid strength degradation, and fracture of the braces. One retrofit alternative for such a bridge pier is to supplement the existing structural system with a system of energy dissipation devices (or structural fuses) that will yield and dissipate energy prior to existing brace buckling. These devices depend on the global shear displacements of the pier to yield and dissipate energy. However, relatively tall and slender bridge piers are also subject to large overturning displacements. This paper investigates and quantifies the effectiveness of using supplemental systems relying on devices used to control pier shear displacements to retrofit braced steel bridge piers, including the effect of overturning displacements on the effective ductility of such systems. A closed form equation for the total ductility of the retrofitted pier, as a function of the shear displacement ductility, is derived and expressed graphically. A simple preliminary design procedure that incorporates these effects is proposed and an example design is presented.

Key Words: Seismic Retrofit, Steel Bridges, Ductility, Overturning, Steel Piers, Unbonded Braces

[1]Corresponding Author, Ph.D. Candidate, Dept. of Civil, Structural, and Environmental Engineering, 212 Ketter Hall, University at Buffalo, Buffalo, NY 14260. Email: jwberman@eng.buffalo.edu Phone: (716)645-2114x2437 Fax: (716)645-3733.

[2]Director, Multidisciplinary Center for Earthquake Engineering Research, and Prof., Dept. of Civil, Structural, and Environmental Engineering, 212 Ketter Hall, University at Buffalo, Buffalo, NY 14260. Email: bruneau@mceermail.buffalo.edu

INTRODUCTION

A large number of long span steel truss bridges were built across the United States at a time when seismic design specifications did not exist. Many of those bridges are located in areas of moderate to high seismicity, and are likely to be subjected to a severe earthquake during their remaining service life. Recent analysis of some of these bridges indicated that they are expected to suffer significant damage and may collapse (Astaneh et al., 1995, Ritchie et al., 1999). Contributing significantly to this undesirable behavior are the latticed built-up members typically used in those structures. These members have been shown to possess little effective ductility prior to fracture (Astaneh et al., 1998, Uang and Kleiser, 1997, Itani et al., 1998, Lee and Bruneau, 2004). While latticed built-up members can be found in the superstructure of these bridges, they are also common in their piers, which tend to be concentrically braced frames, in X or chevron configurations. These piers are critical to the overall seismic performance of steel truss bridges and their bracing members will often fail before other pier or superstructure components. Although concentrically braced frames utilizing monolithic members and having details satisfying the requirements for SCBF (special concetrically braced frames) in the AISC seismic provisions (AISC, 2002) can achieve large ductilities and are used regularly for seismic force resisting systems in buildings, the limited ductility of the latticed braces found in older steel bridge piers inhibit ductile response of the system. As such, retrofit strategies to protect these braces from excessive damage are needed.

One promising retrofit approach is to supplement the existing bracing system with a secondary system that has energy dissipation devices, or structural fuses, designed to yield and dissipate energy prior to the existing braces reaching some limiting relative displacement (see Figure 1).

For the purposes of this paper, structural fuses considered will be limited to steel yielding devices. The effectiveness of such supplemental systems depends on the shear displacement of the pier, Δ_s (Figure 2a), to activate and yield the structural fuses, where the shear displacement of the pier is obtained by summing shear deformations of each panel. However, overturning displacements, Δ_o (Figure 2b), resulting from tension and compression in the pier legs which resist the global overturning moment can also be substantial, particularly in tall and slender bridge piers composed of several panels vertically. These overturning displacements are well known and considered in conventional design. However, their effect on the ductility of systems retrofitted with devices that depend on the inter-panel shear displacements to activate yielding in structural fuses has not been studied.

This paper investigates and quantifies the effectiveness of using supplemental systems relying on devices used to control pier shear displacements to retrofit braced steel bridge piers. This includes the effect of overturing displacements on the effective ductility of such systems. Important parameters are defined in terms of the assumed monotonic behavior of the unretrofitted and retrofitted piers and are used to define the maximum available ductility for the system. General trends regarding the effect of the various parameters on the available ductility are graphically examined and a few special cases are discussed. The practical significance of the results is discussed, a preliminary design procedure for supplemental system retrofits is proposed, a design example is presented, and future research recommendations are given. The results may also be used to determine when a controlled rocking system that relies on overturning displacements to dissipate energy, such as that developed by Pollino and Bruneau (2004), may provide better efficiency than a system dependent on shear displacements.

GENERAL MONOTONIC BEHAVIOR OF EXISTING BRACED STEEL BRIDGE PIERS

Monotonic pushover curves are used here to estimate available ductility. As such, the assumed monotonic behavior of the unretrofitted bridge pier is first defined. Figure 3 shows the assumed behavior, where, K_p is the initial pier stiffness, K_{pb} is the stiffness of the pier after the compression braces buckle, V_{be} and Δ_{be} are respectively, the base shear and pier displacement when the compression braces buckle, V_{ue} and Δ_{ue} are respectively, the base shear and pier displacement when the tension braces yield, Δ_{le} and V_{le} are the limit displacement and corresponding base shear (which are discussed later), and V and Δ_t are the base shear and total displacement, respectively. Note it is also assumed that all the compression braces buckle simultaneously and that all the tension braces yield at the same displacement. This is a reasonable assumption for a bridge pier since the mass is mostly lumped at the top of the pier and typically all the braces are the same size.

The curve of Figure 3 can be constructed from the multiple spring model of Figure 4, with one spring representing the shear stiffness of the existing pier, K_{es}, and one spring representing the overturning stiffness of the pier, K_o. It is assumed that the columns of the pier remain elastic, and that therefore the overturning stiffness is constant. To model brace buckling and yielding, tri-linear shear stiffness is considered, with the post-buckling stiffness expressed as αK_{es}, where α is a factor that can vary from 0 to 1. Figure 5 shows the curve of Figure 3 separated into its shear and overturning components, where, Δ_{bs} and Δ_{bo} are respectively the shear and overturning displacements of the pier when the compression braces buckle, Δ_{us} and Δ_{uo} are the shear and overturning displacements of the pier when the tension braces yield, and Δ_{ls} and Δ_{lo} are the limit shear and overturning displacements of the pier described below. The total displacement is then

the sum of the sum of the shear and overturning displacements. In this case, note that after the existing tension braces yield, the maximum lateral load for the system has been reached, along with the maximum displacement from overturning. Furthermore, since the springs are in series, the total pier stiffness before and after brace buckling are:

$$K_p = \frac{K_{es} K_o}{K_{es} + K_o} \qquad and \qquad K_{pb} = \frac{\alpha K_{es} K_o}{\alpha K_{es} + K_o} \tag{1}$$

Available test data on the inelastic performance of braces in compression in terms of brace axial displacements, can be expressed in terms of pier shear displacements, and correspondingly, a displacement limit for the existing pier can be defined in terms of the shear displacement of the pier at compression brace buckling as:

$$\Delta_{ls} = \kappa \Delta_{bs} \tag{2}$$

where κ is a factor ranging from 1 to Δ_{us}/Δ_{bs}, which keeps the limit displacement less than the displacement at which the tension braces yield. Note that κ would correspond to a maximum allowable "ductility" for the unretrofitted pier, considering only the pier shear deformations, assuming that those deformations are limited to Δ_{ls}, and if the pier "yield" point would be defined as the point at which buckling of the compression braces occurs. Labeling the base shear at the limit displacement as V_l, and noting that the total displacement of the pier is equal to the sum of the shear displacement and the overturing displacement, the total displacement of the pier at the limit brace deformation can be written as:

$$\Delta_l = \Delta_{ls} + \frac{V_{le}}{K_o} \tag{3}$$

and similarly, the pier displacement at brace buckling can be written as:

$$\Delta_b = \Delta_{bs} + \frac{V_{be}}{K_o} \quad \textbf{(4)}$$

Based on data from existing bridge piers and tests on latticed members in compression, appropriate limits for brace deformation, pier shear displacements, and total pier displacements can be found. These can then be compared to the displacement demand, found using the initial stiffness of the pier, K_p.

GENERAL MONOTONIC BEHAVIOR OF RETROFITTED BRACED STEEL BRIDGE PIERS

Consider a case in which the existing pier was found to be inadequate. The retrofit scenario considered here is to supplement the existing bracing system with one that contains a passive energy dissipation device, such as a metallic yielding element. Assume that the retrofit is configured such that the spring system representation of Figure 4 now looks as shown in Figure 6, where, the spring with initial stiffness, K_a, represents the stiffness of the device and any support framing necessary to implement it. Here, it is assumed that the retrofit depends on the shear deformation of the pier to dissipate energy.

The shear stiffness of the existing bracing system and retrofit system act in parallel and their respective base shear vs. displacement curves are shown in Figure 7 (the dotted line is the behavior of the existing frame and the solid line is that of the device, which has been assumed to behave in an elastic-perfectly plastic manner), where V_{ya} is the base shear needed to yield the devices alone, V_{be} is the base shear necessary to buckle the existing braces alone, V_{le} is the base shear at the shear displacement limit of the existing pier (due only to the existing pier), V_{ue} is the

base shear at the shear displacement which causes existing brace yielding (due only to the existing pier), Δ_{ls} is the pier shear displacement limit, and Δ_{ys}, Δ_{bs}, and Δ_{us} are the pier shear displacements which cause yielding of the device, buckling of the existing compression braces, and yielding of the existing tension braces, respectively. Since forces and stiffnesses are additive for these springs in parallel, the pushover curve for the retrofitted pier considering only shear displacements can be constructed as shown in Figure 8a, where the displacements are the same as those in Figure 7, V_l is the total base shear at the pier shear displacement limit, and V_y, V_b, and V_u are the total base shears at device yield, existing compression brace buckling, and existing tension brace yield, respectively.

As shown in Figure 6, the shear displacement dependent device and existing braces are in series with the overturing stiffness of the existing pier, so that the forces through them are the same and the displacements and flexibilities are additive. Therefore, the base shear versus overturning displacement of Figure 8b can be constructed, where Δ_l is the total pier displacement which corresponds to reaching the limit base shear, and Δ_y, Δ_b, and Δ_u are the total pier displacements at device yield, existing compression brace buckling, and existing tension brace yielding, respectively. Finally, the resulting pushover curve for the complete retrofitted pier is shown in Figure 9, where K_1 is the initial stiffness of the system, K_p is the stiffness of the system after the retrofit device has yielded, and K_{pb} is the stiffness of the system after the existing compression braces have buckled. K_p and K_{pb} are as given by Equation (1) and K_1 can be found (knowing that the shear displacement dependent springs are in series with the overturning spring) as:

$$K_1 = \frac{(K_{es}+K_a)K_o}{K_{es}+K_a+K_o} \qquad \textbf{(3)}$$

DUCTILITY OF RETROFITTED BRACED STEEL BRIDGE PIERS

Using the above pushover curves, the maximum available ductility of the retrofitted pier can be assessed. Considering the limit shear displacement of the pier, Δ_{ls}, which could be established from a review of existing experimental results, the maximum available ductility in terms of pier shear displacement is:

$$\mu_{maxs} = \frac{\Delta_{ls}}{\Delta_{ys}} \tag{4}$$

Note that this quantity is also the maximum local ductility demand on the device itself, assuming that the limit displacement is not exceeded and that the flexibility of support framing for the device can be neglected. Similarly, the maximum available global or total ductility, μ_{max}, can be written as:

$$\mu_{max} = \frac{\Delta_l}{\Delta_y} \tag{5}$$

where Δ_l and Δ_y are total displacements. Still needing to be established is the corresponding level of global ductility for a given maximum ductility in terms of shear displacements.

From Figures 8 and 9, the total limit displacement can be written as:

$$\Delta_l = \Delta_{ls} + \frac{V_l}{K_o} \tag{6}$$

where, $\Delta_{ls} = \kappa\Delta_{bs}$ as defined previously. Note that Equation (6) is the same as Equation (3) for the unretrofitted pier except that V_l has replaced V_{le}. Similarly, the total displacement when the retrofit device yields can be written as:

$$\Delta_y = \Delta_{ys} + \frac{V_y}{K_o} \tag{7}$$

The base shear at the limit displacement can be written from Figure 7 as:

$$V_l = V_{le} + V_{ya} = \Delta_{ys} K_a + \Delta_{bs} K_{es} + \alpha K_{es}\left(\Delta_{ls} - \Delta_{bs}\right) \tag{8}$$

Substituting $\Delta_{ls} = \kappa\Delta_{bs}$ into Equation (8) and rearranging gives:

$$V_l = \kappa \Delta_{bs}\left[\frac{\Delta_{ys} K_a}{\kappa \Delta_{bs}} + K_{es}\left(\frac{1}{\kappa} + \alpha - \frac{\alpha}{\kappa}\right)\right] \tag{9}$$

Inserting Equation (9) into Equation (6) leads to:

$$\Delta_l = \kappa \Delta_{bs}\left[1 + \frac{\Delta_{ys} K_a}{\kappa \Delta_{bs} K_o} + \frac{K_{es}}{K_o}\left(\frac{1}{\kappa} + \alpha - \frac{\alpha}{\kappa}\right)\right] \tag{10}$$

which, recalling the definition of shear displacement ductility in Equation (4), results in the following equation for the total limit displacement:

$$\Delta_l = \kappa \Delta_{bs}\left[1 + \frac{1}{\mu_{maxs}}\frac{K_a}{K_o} + \frac{K_{es}}{K_o}\left(\frac{1}{\kappa} + \alpha - \frac{\alpha}{\kappa}\right)\right] \tag{11}$$

From Figure 8a, the yield base shear, V_y, can be written as:

$$V_y = \Delta_{ys}\left(K_a + K_{es}\right) \tag{12}$$

and inserting this into Equation (7) gives:

$$\Delta_y = \Delta_{ys}\left[1 + \frac{K_a}{K_o} + \frac{K_{es}}{K_o}\right] \tag{13}$$

Defining the stiffness ratios, η and λ as:

$$\eta = \frac{K_{es}}{K_o} \qquad \textit{and} \qquad \lambda = \frac{K_a}{K_o} \tag{14}$$

and inserting these and Equations (11) and (13) into Equation (5) gives the maximum available global ductility:

$$\mu_{max} = \mu_{maxs}\left[\frac{1+\frac{\lambda}{\mu_{maxs}}+\eta\left(\frac{1}{\kappa}+\alpha-\frac{\alpha}{\kappa}\right)}{1+\lambda+\eta}\right] \quad \textbf{(15)}$$

As evidenced by Equation (15), the maximum available global ductility depends not only on the pier shear ductility, but also the stiffness ratios, α, η, and λ, and the ratio of the limiting existing brace displacement to its buckling displacement, κ. Furthermore, since κ and μ_{maxs} were defined to be greater than or equal to 1, and α was defined to be between 0 and 1, it can be shown that the factor multiplying μ_{maxs} on the right side of Equation (15) is always less than or equal to 1, indicating that the maximum available global ductility of the system is always less than the maximum available ductility neglecting overturning displacements.

To prevent premature device failure, it is important to ensure that device ductile capacities, for the device chosen, are not exceeded. As noted above, if the flexibility of any support framing for the retrofit device can be neglected, the shear ductility is equivalent to the device ductility. However, in cases where the support framing for the device is flexible and has a stiffness K_s, and the device has a stiffness K_d, the stiffness of the device and support framing, K_a, is:

$$K_a = \frac{K_d K_s}{K_d + K_s} \quad \textbf{(16)}$$

and the device ductility, μ_d, can be written in terms of the pier shear ductility as:

$$\mu_d = \mu_{maxs} + (\mu_{maxs} - 1)\frac{K_d}{K_s} \quad \textbf{(17)}$$

This corresponds to another reduction in available ductility, since the pier shear ductility may now be less than the ductility of the device. However, this latter effect is typically accounted for in seismic design.

EXAMINATION OF MAXIMUM AVAILABLE GLOBAL DUCTILITY

Figures 10 through 12 show how the maximum available global ductility, normalized by μ_{maxs}, varies with respect to α, η, λ, and κ, for values of μ_{maxs} of 2, 4, and 6 respectively. From these figures and Equation (15) it is clear that there is a linear variation of μ_{max} with respect to each of the parameters. Additionally, if the overturning stiffness is considered infinite (which is the assumption used when the overturning displacements are neglected), Equation (15) simplifies into that for the maximum available pier shear ductility. Also, it is evident from these figures that the difference between the maximum available ductility neglecting overturning displacements and the maximum available ductility considering overturning displacements can be significant, in some cases, the latter being as little as one half the former.

There are several observations that can be made regarding the efficiency of retrofit solutions based on Figures 10 through 12, where efficiency may be thought of as the ratio of global maximum ductility to the maximum shear displacement ductility. First, if the maximum available shear ductility is increased, say from 2 to 4, while all other parameters remain constant, the increase in the maximum available global ductility increases by a factor less than 2. For example, consider a bridge pier with stiffness ratios, η and λ equal to 1, an existing pier second slope stiffness ratio, α, of 0.25, and an existing brace displacement factor, κ, of 1.5. For a maximum shear displacement ductility of 2, the maximum corresponding global ductility is 1.5.

If, for the same system, the maximum shear displacement ductility is increased to 4, the maximum global ductility becomes 2.7. Although the actual value of global ductility is larger, there is a larger decrease in maximum ductility, indicating that the system would not be using the yielding device as efficiently.

Another general observation is that systems with larger α values (which is the second slope shear stiffness ratio for the unretrofitted pier) have global ductility ratios that are closer to the shear displacement ductility ratios. In other words, systems in which the post-buckling strength degradation of the existing braces is smaller, have a smaller reduction in ductility due to overturing displacements.

SPECIAL CASES

It is worthwhile to consider some special cases where Equation (15) can be simplified. First, consider the case where the limiting shear displacement of the pier corresponds to brace buckling. In this case, κ is 1, and Equation (15) becomes:

$$\mu_{max} = \mu_{maxs}\left[\frac{1+\frac{\lambda}{\mu_{maxs}}+\eta}{1+\lambda+\eta}\right] \tag{18}$$

which logically is no longer a function of the post-buckling shear stiffness of the unretrofitted pier. Note that when the limiting displacement is taken as the buckling displacement, the required yield displacement of the supplemental system devices to achieve the seismic performance objectives may be prohibitively small.

A second interesting special case occurs when the existing unretrofitted pier is considered to behave as an elastic perfectly plastic system, i.e., $\alpha = 0$. Here, Equation (15) reduces to:

$$\mu_{max} = \mu_{maxs}\left[\frac{1+\frac{\lambda}{\mu_{maxs}}+\frac{\eta}{\kappa}}{1+\lambda+\eta}\right] \quad \textbf{(19)}$$

This could be representative of bridge pier systems that are not necessarily braced frames (i.e. portal frames), or tension-only braced frames. In this case, the limit base shear is also the base shear at which the existing framing yields and maximum capacity of the retrofitted pier. Therefore, under the assumption of an elastic perfectly plastic unretrofitted pier, displacements due to overturning do not contribute to the total displacement of the pier after the existing system yield displacement has been reached.

Finally, in new construction in which a fuse type element that depends on the global shear displacements of the pier to dissipate energy and provide ductility is used, $\eta = 0$. In this case, the pier pushover curve is bilinear, the base shear at device yield and base shear at the limit displacement are equal, and overturning displacements do not increase above those base shear levels. As a result; the difference in maximum available ductility when neglecting or considering overturing displacements is due only to the difference in the yield displacement for those two scenarios. In other words, the difference between μ_{maxs} and μ_{max} when $\eta = 0$, is related to the difference between Δ_y and Δ_{ys}. Equation (15), in this case, reduces to:

$$\mu_{max} = \mu_{maxs}\left[\frac{1+\frac{\lambda}{\mu_{maxs}}}{1+\lambda}\right] \quad \textbf{(20)}$$

Equation (20) can be thought of as the result for two-springs in series, in which the springs represent the nonlinear shear displacement dependant device, and the linear overturning. This is

the same concept as that used for the development of local versus global ductility demands for simple bridges as derived in (Alfawakhiri and Bruneau, 2000). However, there the relationship derived was not for a system subject to large overturing displacements, but for a fuse element and a protected element. Here we see that in this special case, results obtained following the two approaches are equivalent.

DESIGN SPECTRUM

The seismic force modification factor, R, used, along with the design spectrum, to calculate the design base shear for a given structure's period is taken here as the product of the system overstrength, Ω_o, and the ductility factor, R_μ, where:

$$R_\mu = \begin{matrix} 1 \\ \sqrt{2\mu - 1} \\ \mu \end{matrix} \quad for \quad \begin{matrix} T_n < T_a \\ T_b < T_n < T_c \\ T_c < T_n \end{matrix} \tag{21}$$

T_a is 0.03 seconds, T_b is 0.15 seconds, T_c is 0.5 seconds, and T_n is the natural period of the structure found using the initial stiffness (Newmark and Hall, 1982). Some design codes use the periods T_o and T_s, as T_b and T_c, where T_o and T_s are found from the ordinates of the design spectrum as:

$$T_o = 0.2\frac{S_{DS}}{S_{D1}} \qquad and \qquad T_s = \frac{S_{DS}}{S_{D1}} \tag{22}$$

where S_{DS} is the short period design spectral acceleration and S_{D1} is the 1-second design spectral acceleration.

To determine the appropriate value for the overstrength factor for the retrofitted steel truss bridge pier of interest here, consider Figure 13. Here the "fully yielded" base shear is considered to be

the limit base shear, V_l, and the base shear at which the first plastic hinge forms is the yield base shear, V_y (the base shear at which the retrofit device yields). The conventional definition of the overstrength factor in this case gives:

$$\Omega_o = \frac{V_l}{V_y} \tag{23}$$

Using the above, a simple preliminary design procedure for supplemental system retrofit of steel bridge piers, based on the equivalent lateral load method, is developed and presented below. Although steel truss bridges are often essential lifelines for which nonlinear time history analysis will be performed, a preliminary design procedure can provide engineers with an expedient way to start the retrofit design, and provide insight into how efficient that retrofit will be in terms of maximum shear strength and total ductility.

PRELIMINARY DESIGN PROCEDURE FOR SUPPLEMENTAL RETROFIT OF STEEL TRUSS BRIDGE PIERS

Assume that a steel truss bridge pier is to be retrofitted to protect, or limit the inelastic deformations of, the latticed built-up brace members. Suppose the unretrofitted bridge pier is determined to have the monotonic behavior shown in Figures 3, 4, and 5 and that the brace axial deformation limit is set so that $\Delta_{ls} = \kappa\Delta_{bs}$. Also, assume that the natural period of both the retrofitted and unretrofitted pier (found using the initial total stiffness) is in the constant velocity region of the spectrum, which is generally the case for these bridges. The design base shear for the equivalent lateral load procedure, V_d, is:

$$V_d = \frac{S_a}{R} W = \frac{S_{D1}}{R T_{pr}} W \quad \textbf{(24)}$$

where, S_a is the spectral acceleration for the assumed damping level and soil type (for a bare steel bridge pier, 2% damping is assumed), R is the seismic force modification factor as defined above, T_{pr} is the retrofitted pier period found using the initial stiffness, K_1, and W is the weight applied at the top of the pier. The proposed design procedure is shown in Figure 14 as a flowchart and descried in the following paragraphs.

The first step is to assume a value for the seismic force modification factor, R. Then the required yield base shear, for the assumed value of R can be calculated from Equation (24), where the design base shear is the yield base shear, in accordance with Figure 13, and the retrofitted pier period, T_{pr}, can be initially approximated by the unretrofitted pier period. Next, the yield base shear for the device only, V_{ya}, and the pier shear displacement at device yield, Δ_{ys}, are selected such that they satisfy:

$$V_y = V_{ya} + \Delta_{ys} K_f \quad \textbf{(25)}$$

where K_f is the shear stiffness of the existing frame. Recommended initial values for V_{ya} and Δ_{ys} are $0.5V_{be}$ and $0.5\Delta_{bf}$, respectively. These values ensure that the devices yield before the existing braces buckle. From these, the shear stiffness of the retrofit (including any support framing) can be calculated as:

$$K_a = \frac{V_{ya}}{\Delta_{ys}} \quad \textbf{(26)}$$

Next, the initial stiffness of the retrofitted pier, and corresponding period can be calculated using Equation (3). The stiffness ratios η and λ, as well as the shear ductility can then be found using Equations (14) and (4) respectively, and are used to estimate the maximum total ductility, μ_{max}, as given by Equation (15). Then the value for the limit base shear, V_l, is determined by constructing the pushover curve for the system, or if the limit base shear for the unretrofitted structure, V_{le}, was determined previously, V_l can be found from $V_l = V_{le} + V_{ya}$. Finally, the corresponding overstrength and ductility factors, Ω_o and R_μ, from Equations (21) and (23), and multiplied to give seismic force modification factor. This factor and the updated pier period are then used to begin a second iteration with Equation (24). Alternatively, if the effective R obtained per the above calculations exceeds the R assumed, it is possible to simply recalculate the period of the pier and make sure the corresponding yield base shear still exceeds the design base shear (Equation 24) for the effective R (although this option is not shown in Figure 14). Note that further iterations will provide a more efficient design, i.e., the brace deformations will more closely approach the limit values.

EXAMPLE: SUPPLEMENTAL RETROFIT OF A STEEL TRUSS BRIDGE PIER

To illustrate the above design procedure, consider a three story steel x-braced pier with a width of 7.32 m and story (or panel) height of 7.32 m as shown in Figure 15. This pier, and its member properties, have been developed as a result of a survey of several actual steel truss bridges in the United States and Canada. It represents the pier of a smaller bridge that would carry two lanes of traffic. The pier columns have a cross-sectional area of 1.56×10^4 mm^2 and are equivalent to W 360 x 122 (W 14 x 82), the braces and horizontal members have cross-sectional areas of 3.55×10^3 mm^2, and the pier carries a gravity weight of 1110 kN, half of which can be lumped at the top

of each column. Using these dimensions the pier has a overturning moment of inertia of 0.416 m^4. Assume the existing braces have a yield stress of 250 MPa and that their buckling capacity is ½ of their tensile capacity (corresponding to a yield strength of 880 kN and buckling strength of 440 kN). Furthermore, assume that the strength of the compression braces after buckling degrades at a rate equal to the negative of their initial stiffness and that the braces are elastic-perfectly plastic in tension. For modeling expediency, in this case, the same panel inelastic behavior can be obtained by considering each brace as an elastic-perfectly plastic element with equal positive and negative "yield" strengths of 440 kN. As a result, the maximum base shear for the unretrofitted pier is 623 kN, and the existing pier itself exhibits an elastic-perfectly plastic behavior up to the actual yielding displacement of the existing brace, after which the behavior is not defined. The limit deformation of the existing braces has been set to 1.5 times their buckling displacement (the axial buckling deformation is 6.4 mm and limit axial deformation is 9.6 mm for a Young's Modulus of 2×10^5 MPa).

Using the above information, the behavior of the existing pier is summarized in Table 1 (with the parameters corresponding to those shown in Figures 3 and 5). Assume the pier demand has been determined using the design spectrum given in MCEER/ATC 49 (ATC/MCEER, 2003), which is equivalent to the one given in FEMA 368 (FEMA, 2000), and has a S_{DS} of 1.5g and a S_{D1} of 0.6g. Using the equal displacement rule assumption, the spectral displacement for the unretrofitted pier may be used to estimate the maximum displacement of the pier as 93 mm. The limit displacement of the pier, given in Table 1, is 67 mm, indicating that the pier needs to be retrofitted. A supplemental system relying on unbonded braces to dissipate energy, similar to Figure 1, is chosen for this retrofit.

Assuming an R of 2, the required yield base shear is found to be 537 kN from Equation (24). Using $\Delta_{ys} = 0.5\Delta_{bs}$ and $V_{ya} = 0.4V_{be}$ gives a V_y of 560 kN according to Equation (25). The retrofit shear stiffness, K_a, total pier stiffness, K_1, and retrofitted pier period, T_{pr}, are then 18.3 kN/mm, 15 kN/mm, and 0.55 sec, respectively. Stiffness ratios, η and λ, are 0.97 and 0.78, and the maximum available shear ductility, μ_{maxs}, is 3. Using these in Equation (15) gives a maximum available total ductility, μ_{max}, of 2.1. Adding the unretrofitted limit base shear, V_{le}, to the device yield base shear, V_{ya}, gives the new limit base shear, V_l, of 872 kN, and overstrength factor of 1.56. The resulting seismic force modification factor is 3.24, which exceeds the initially assumed value of 2. Updating this and the period gives a required yield base shear of 377 kN. While further iterations are possible, (i.e., to find retrofit parameters for this updated yield base shear), here, design is deemed satisfactory since the values obtained for the above parameters achieve the objective of limiting the existing brace deformation. Using the required shear stiffness, K_a, shear yield displacement, Δ_{ys}, and device base shear, V_{ya}, of the retrofit from above, the unbonded braces and support structure were designed. Unbonded brace areas of 363 mm^2, lengths of 1.52 m, and yield stresses of 345 MPa were selected and the braces were assumed to be oriented horizontally, with new supplemental HSS 254x254x15.9 inverted chevron braces supporting them. Resulting axial yield force and deformation for the unbonded braces were 125 kN and 2.6 mm respectively. The system properties (corresponding to Figures 7, 8, and 9) are given in Table 1 and the corresponding R value is 3.4 using the specified unbonded brace and support structure sizes. From these properties, and assuming again that the equal displacement rule applies, the displacement demand on the pier using the MCEER/ATC 49 spectrum is found to be 81.2 mm, which is just slightly larger than the new limit displacement from Table 1 of 77.8 mm. However, since the retrofitted pier now has a tri-linear pushover curve the equal

displacement rule may provide a less accurate approximation of the maximum displacement as compared to a system with a bilinear pushover curve. For this reason time history analyses were also performed as described below.

Nonlinear time history analyses were conducted on a models of the unretrofitted and retrofitted piers using Sap2000 (CSI, 1997). Existing braces were modeled as axially yielding elastic-perfectly plastic link elements, with small flexural stiffnesses (to mimic pinned end connections), and compressive and tensile yield displacements and axial loads set to the buckling values as described above. In the retrofitted pier model, the unbonded braces were modeled as elastic perfectly-plastic with the axial yield force and deformation values calculated above. Three spectrum compatible synthetic earthquake records, generated using the program RSCTH (RSCTH, 1999), and the ground motion component TEM090, LA-Temple and Hope station, of the 1994 Northridge earthquake (amplitude scaled to a 0.55 sec spectral acceleration of 1.14g to match the target spectrum) were used as acceleration time histories for both the retrofitted and unretrofitted pier models (PEER, 2000). The acceleration time histories and acceleration response spectrums are shown in Figures 16 and 17 (the target response spectrum, using the ordinates given above, is also shown in Figure 17).

The existing braces of the unretrofitted pier model were subjected to a maximum axial deformation of 15.8 mm, which occurred under the selected TEM090 scaled motion and is more than 1.6 times their limit deformation. A maximum base shear of 623 kN and maximum pier displacement of 104.5 mm were obtained for the same ground motion.

For the retrofitted pier, the maximum deformation of the existing braces was successfully limited to 7.5 mm, which occurred under the selected TEM090 scaled motion, and is significantly less than the 1.5 times the buckling deformation limit (9.6 mm). A maximum base shear of 864 kN and maximum pier displacement was obtained under that same motion. The unbonded brace elements underwent peak axial deformations of 13 mm, indicating a local ductility demand of 5, which unbonded braces have been shown capable to achieve (Iwata et al., 2000). Note that from Equation (17), for the design maximum available shear ductility and supplementary system considered, the maximum local ductility demand on the braces was expected to be 6.8, which is also within the range of satisfactory performance for unbonded braces. This retrofit design, therefore, achieved the objective of limiting the deformation of the existing braces. As mentioned above, further iterations during the design procedure would bring the existing brace deformations closer to the specified limit.

Connection of this particular supplemental system to the existing pier could be achieved through the addition of gussets at the connections of the existing braces to the existing columns. The unbonded braces as well as their support braces could connected to the gussets while the gussets are connected to the columns of the pier. In certain cases, column retrofit may also be necessary to handle the increased strength demands the brace retrofit places on them. However, previous research had indicated that the latticed braces were indeed the crucial weak elements in these piers. While these retrofits and connections to the existing frames are costly, they may be more economical than pier replacement which may be the only other alternative. These issues will certainly need consideration in the future development of these supplemental retrofit systems.

RECOMMENDATIONS FOR FUTURE RESEARCH

The analytical study and design procedure presented above for supplemental system retrofit of steel truss bridge piers have been verified using nonlinear time history analysis of a representative pier for three spectrum compatible ground motions. However, the interaction of the retrofitted pier and the bridge superstructure is important and should be addressed in future research using nonlinear time history analysis of entire bridge structures. Furthermore, experimental verification of the performance of such retrofitted systems, both the pier and the entire bridge structure, are likely necessary to provide the confidence necessary to implement such retrofit systems in practice. This paper has provided a basis for such future research and applications.

CONCLUSIONS

A retrofit alternative for steel truss bridge piers in which the latticed built-up bracing members are determined to be critical was introduced. The alternative was denoted a supplemental system, and involves supplementing the existing bracing system with another system that provides added stiffness, strength, and energy dissipation. This supplemental system acts in parallel with the existing bracing and introduces energy dissipation devices having elastic-perfectly plastic behavior. The effect of overturing deformations on such steel truss bridge piers retrofitted with supplemental systems has been considered and shown to reduce maximum available ductility of the system. Equations relating the maximum ductility available to the ductility available when only the shear deformations of piers are considered were derived for various conditions. The sensitivity of the maximum available ductility to parameters such as pier stiffness ratios (including the ratio of the retrofit shear stiffness to the pier overturning stiffness, the ratio of

unretrofitted pier shear stiffness to pier overturning stiffness, and the ratio of unretrofitted shear stiffness after brace buckling to the pier's initial shear stiffness), and allowable existing brace deformation, was presented graphically. A preliminary design procedure was developed and illustrated with a numerical example. Nonlinear time history analysis of the design example indicated that design objectives were met.

The above indicates that supplemental systems are a viable retrofit option for steel truss bridge piers in which removal of the existing latticed built-up members is not possible. Through the use of properly designed energy dissipation devices (or structural fuses), these systems can adequately dissipate energy and provide additional stiffness, such that the deformations of the existing braces are kept below specified levels.

ACKNOWLEDGMENTS

This research was conducted by the State University of New York at Buffalo and was supported by the Federal Highway Administration under contract number DTFH61-98-C-00094 to the Multidisciplinary Center for Earthquake Engineering Research. However, any opinions, findings, conclusions, and recommendations presented in this paper are those of the authors and do not necessarily reflect the views of the sponsors.

REFERENCES

AISC. *Seismic Provisions for Structural Steel Buildings*. American Institute of Steel Construction, Chicago, IL, 2002.

ATC/MCEER. *NCHRP 12-49 Recommended LRFD Guidelines for the Seismic Design of High-way Bridges*, *Part I: Specifications*, ATC/MCEER Joint Venture 2003; Multidisciplinary Center for Earthquake Engineering Research: State University of New York at Buffalo, Buffalo, NY.

Alfawakhiri, F., and Bruneau, M. Flexibility of Superstructures and Supports in the Seismic Analysis of Simple Bridges. *Earthquake Eng Struc* 2000; **29**; 5; 711-729.

Astaneh, A., Shea, J.H., and Cho, S.W. (1995) Seismic Behavior and Retrofit Design of Steel Long Span Bridges, in *Proceedings of the National Seismic Conference on Bridges and Highways: Progress in Research and Practice*, San Diego, CA, Dec. 10-13.

Astaneh, A. Proof-Testing of Latticed Members and their Connections on the San Francisco-Oakland Bay Bridge, *Technical Report UCB/CEE-STEEL-98/03* 1998, Department of Civil and Environmental Engineering, University of California Berkeley, Berkeley, CA.

CSI. *SAP2000 Reference Manual*, Computers and Structures, Inc., Berkeley, CA, 1997.

FEMA. *NEHRP Recommended Provisions for Seismic Regulations for New Buildings and Other Structures*, FEMA 356; Building Seismic Safety Council for the Federal Emergency Management Agency: Washington, D.C., 2000.

Itani, A., Vesco, T., and Dietrich, A. Cyclic Behavior of "As-Built" Laced Members with End Gusset Plates on the San Francisco-Oakland Bay Bridge, *Technical Report CCEER 98-01* 1998, Center for Civil Engineering Earthquake Research, University of Nevada, Reno.

Iwata, M., Kato, T., Wada, A. Buckling-restrained braces as hysteretic dampers. *Proceedings of STESSA 2000 - Third International Conference on the Behaviour of Steel Structures in Seismic Areas*, August, 2000, 33-38, A. A. Balkema, Rotterdam, Nagoya.

Lee, K. and Bruneau, M. Seismic Vulnerability Evaluation of Axially Loaded Steel Built-up Laced Members, *MCEER Technical Report 04-007* 2004, Multidisciplinary Center for Earthquake Engineering Research: State University of New York at Buffalo, Buffalo, NY.

Newmark, N. M., and Hall, W. J. *Earthquake Spectra and Design*, EERI Monograph 3; Earthquake Engineering Research Institute, Oakland, CA., 1982.

PEER. *PEER Strong Motion Database*, (http://peer.berkeley.edu/smcat/index.html) Pacific Earthquake Engineering Research Center: University of California Berkeley, Berkeley, CA, 2000.

Pollino, M., and Bruneau, M. Seismic Retrofit of Bridge Steel Truss Piers Using a Controlled Rocking Approach, *Technical Report MCEER-04-0011* 2004, Multidisciplinary Center for Earthquake Engineering Research, State University of New York at Buffalo, Buffalo, NY.

Ritchie, P., Kauhl, N. and Kulicki, J. Critical Seismic Issues for Existing Steel Bridges, *Technical Report MCEER-99-0013* 1999, Multidisciplinary Center for Earthquake Engineering Research: State University of New York at Buffalo, Buffalo, NY.

RSCTH. *Response Spectrum Compatible Time Histories*, Engineering Seismology Laboratory (http://civil.eng.buffalo.edu/engseislab/index.htm), Multidisciplinary Center for Earthquake Engineering Research: State University of New York at Buffalo, Buffalo, NY.

Uang, C.M., and Kleiser, M. Cyclic Performance of As-Built Latticed Members for the San Francisco-Oakland Bay Bridge, *Report No. SSRP-97-01* 1997 , Department of Structural Engineering, University of California, San Diego.

Table 1 Properties of Example Unretrofitted and Retrofitted Piers

Displacements (mm)								
Pier	Δ_{ys}	Δ_{bs}	Δ_{ls}	Δ_{us}	Δ_{y}	Δ_{b}	Δ_{l}	Δ_{u}
Unretrofitted	N.A.	27.2	40.9	54.5	N.A.	53.6	67.2	80.9
Retrofitted	13.2	27.2	40.9	54.5	36.6	64.2	77.8	91.4
Base Shear (kN)								
Pier	V_{ya}	V_{be}	V_{le}	V_{ue}	V_{y}	V_{b}	V_{l}	V_{u}
Unretrofitted	N.A.	623	623	623	N.A.	623	623	623
Retrofitted	250	623	623	623	552	873	873	873
Stiffnesses (kN/mm)								
Pier	K_a	K_{es}	αK_{es}	(K_a+K_{es})	K_o	K_1	K_p	K_{pb}
Unretrofitted	N.A.	22.9	0	N.A.	23.6	N.A.	11.6	0
Retrofitted	19.0	22.9	0	41.8	23.6	15.1	11.6	0

Figure Captions for "Supplemental System Retrofit Considerations for Braced Steel Bridge Piers" by Jeffrey W. Berman and Michel Bruneau.

Figure 1 Schematic of Supplemental System Retrofit Approach

Figure 2 (a) Pier Shear Displacement (b) Pier Overturing Displacement

Figure 3 Assumed Unretrofitted Pier Pushover Curve

Figure 4 Two Spring Representation of Unretrofitted Pier

Figure 5 (a) Pier Shear Displacement Pushover Curve (b) Pier Overturing Displacement Pushover Curve

Figure 6 Three Spring Model of Retrofitted Pier

Figure 7 Shear Displacement Pushover Curves for Device and Existing Pier

Figure 8 (a) Retrofitted Pier Shear Displacement Pushover Curve (b) Retrofitted Pier Overturing Displacement Pushover Curve

Figure 9 Retrofitted Pier Pushover Total Curve

Figure 10 μ_{max}/μ_{maxs} for $\mu_{maxs} = 2$

Figure 11 μ_{max}/μ_{maxs} for $\mu_{maxs} = 4$

Figure 12 μ_{max}/μ_{maxs} for $\mu_{maxs} = 6$

Figure 13 Retrofitted Pier Pushover Curve with Elastic Response

Figure 14 Flow Chart for Supplemental System Preliminary Design Procedure

Figure 15 Schematic of Unbonded Brace (UBB) Supplemental System Retrofit Example

Figure 16 Acceleration Time Histories

Figure 17 Acceleration Response Spectra

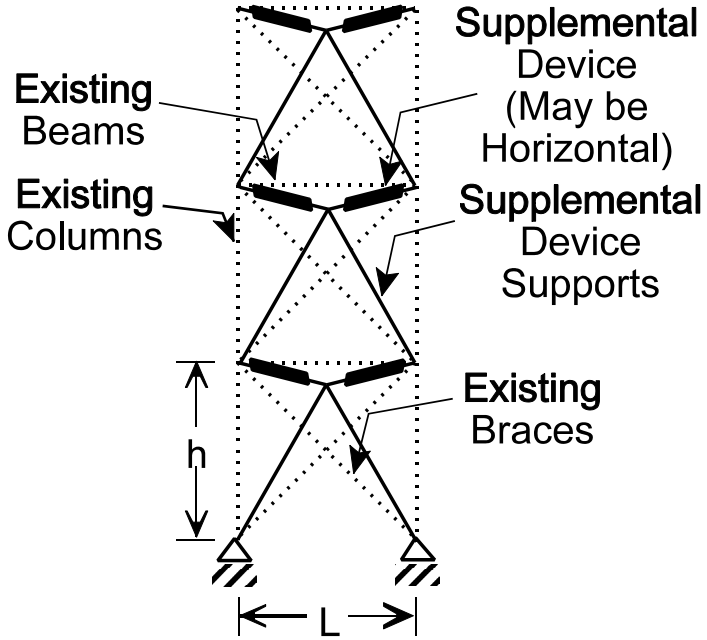

Figure 1 Schematic of Supplemental System Retrofit Approach

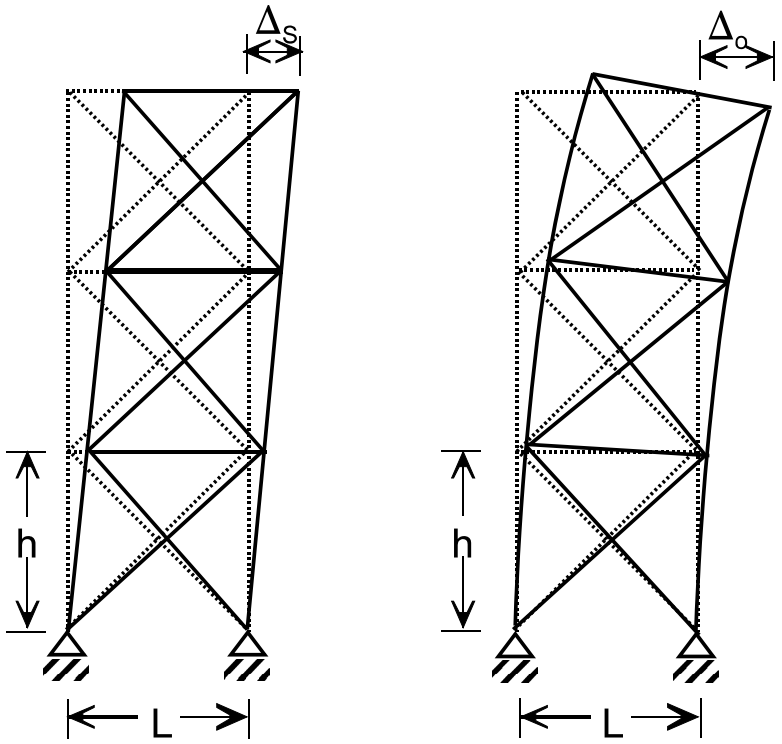

Figure 2 (a) Pier Shear Displacement (b) Pier Overturing Displacement

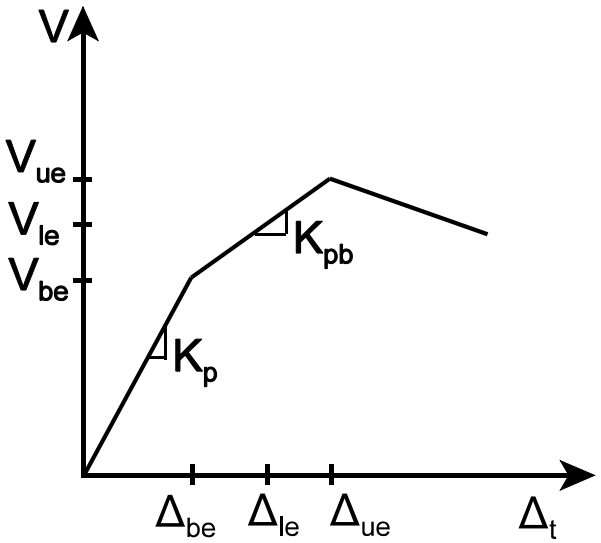

Figure 3 Assumed Unretrofitted Pier Pushover Curve

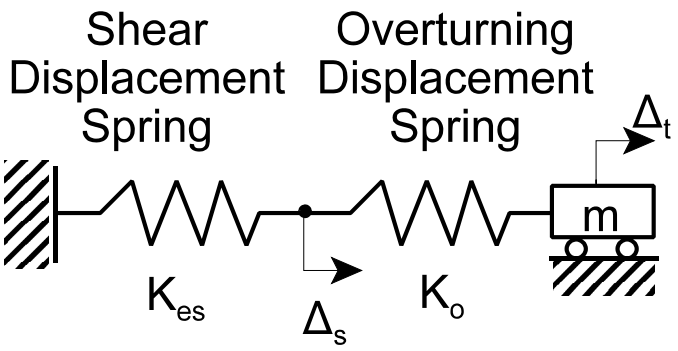

Figure 4 Two Spring Representation of Unretrofitted Pier

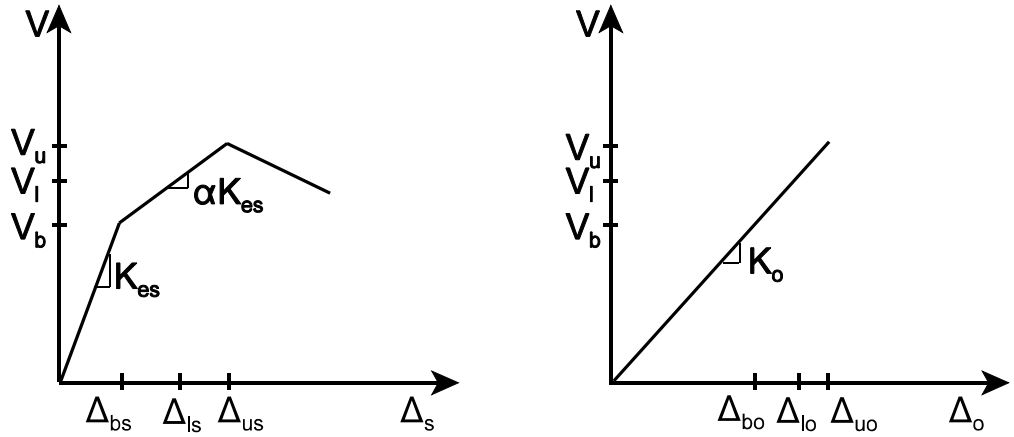

Figure 5 (a) Pier Shear Displacement Pushover Curve (b) Pier Overturing Displacement Pushover Curve

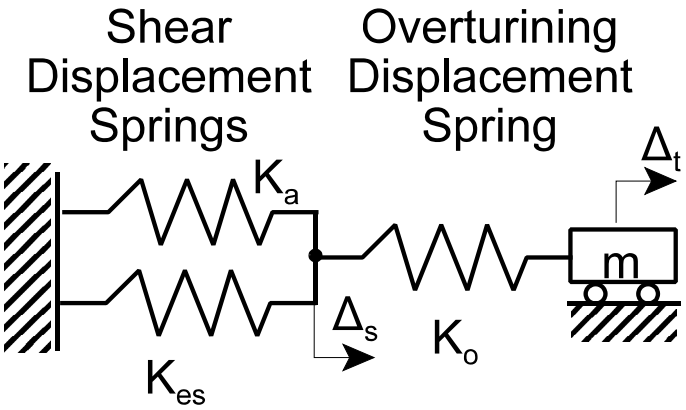

Figure 6 Three Spring Model of Retrofitted Pier

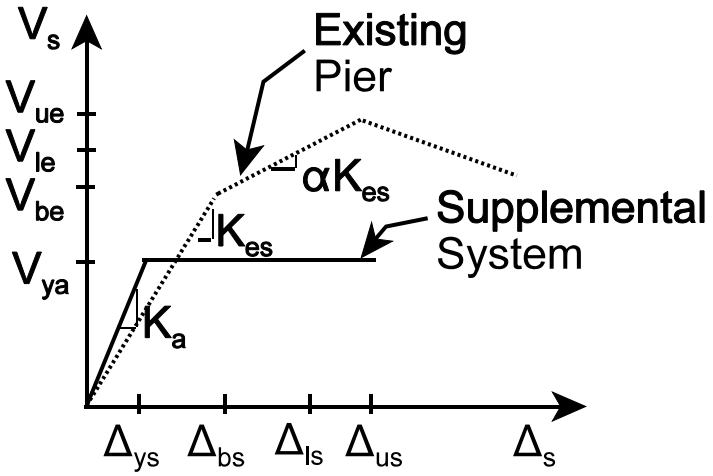

Figure 7 Shear Displacement Pushover Curves for Device and Existing Pier

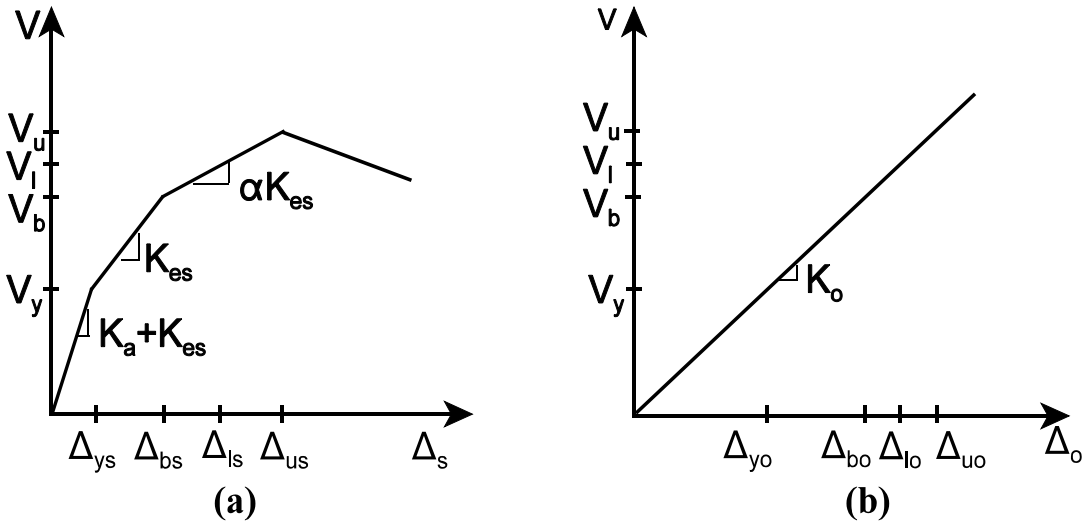

Figure 8 (a) Retrofitted Pier Shear Displacement Pushover Curve (b) Retrofitted Pier Overturing Displacement Pushover Curve

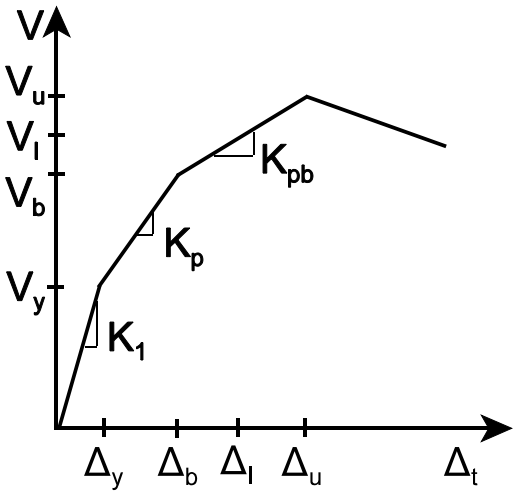

Figure 9 Retrofitted Pier Pushover Total Curve

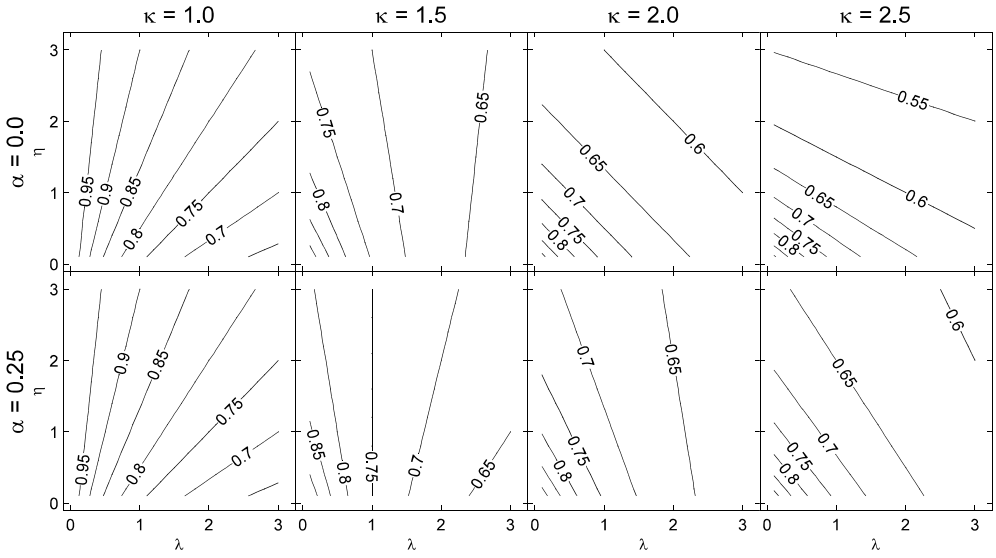

Figure 10a μ_{max}/μ_{maxs} for $\mu_{maxs} = 2$

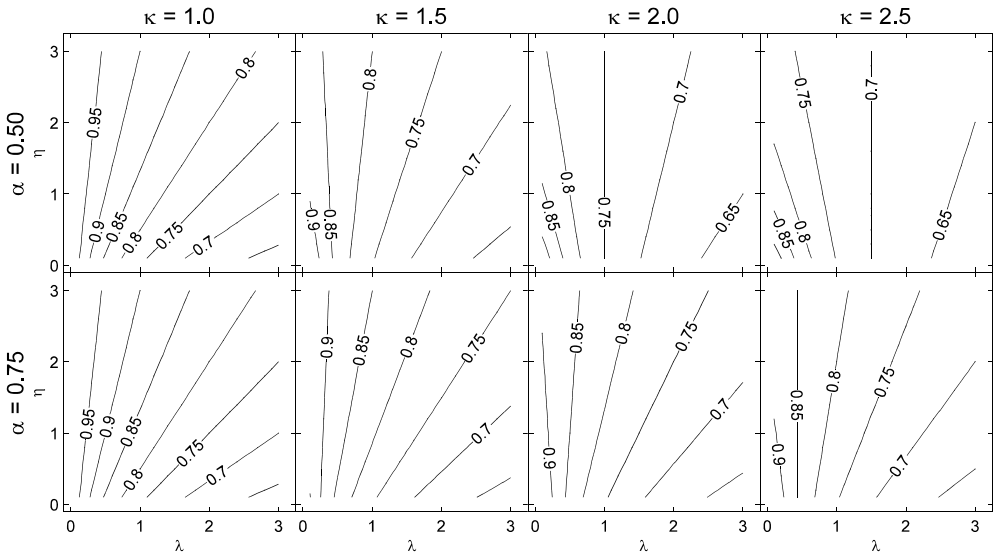

Figure 10b μ_{max}/μ_{maxs} for $\mu_{maxs} = 2$

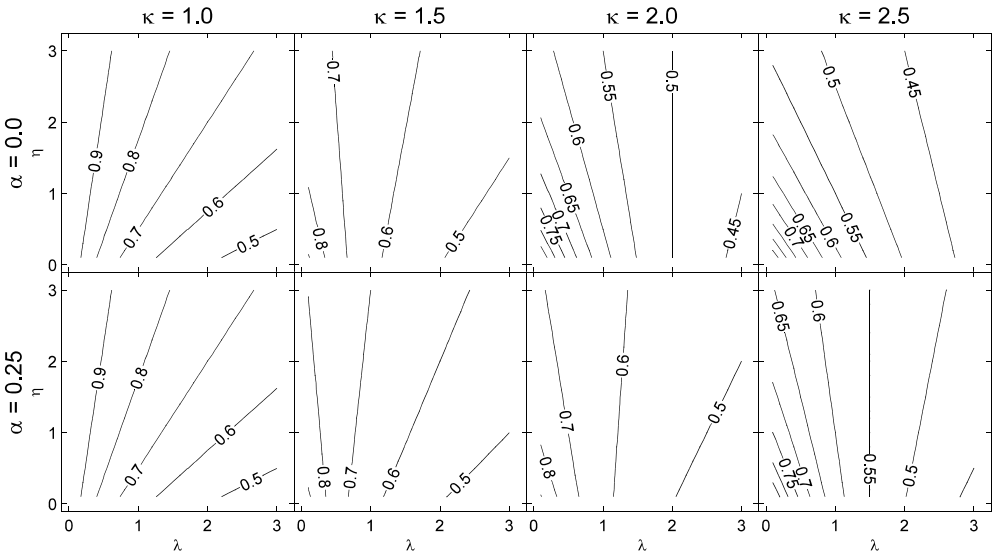

Figure 11a μ_{max}/μ_{maxs} for $\mu_{maxs} = 4$

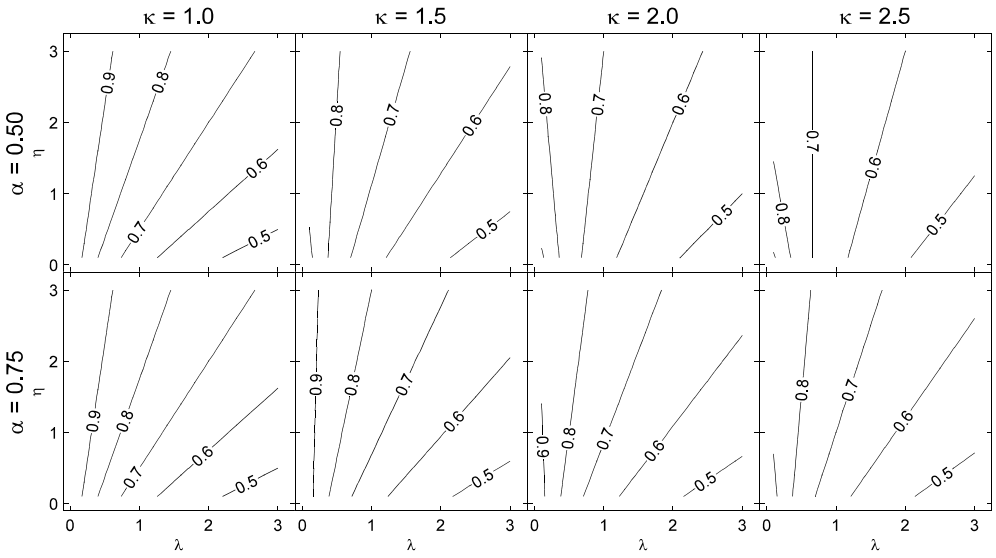

Figure 11b μ_{max}/μ_{maxs} for $\mu_{maxs} = 4$

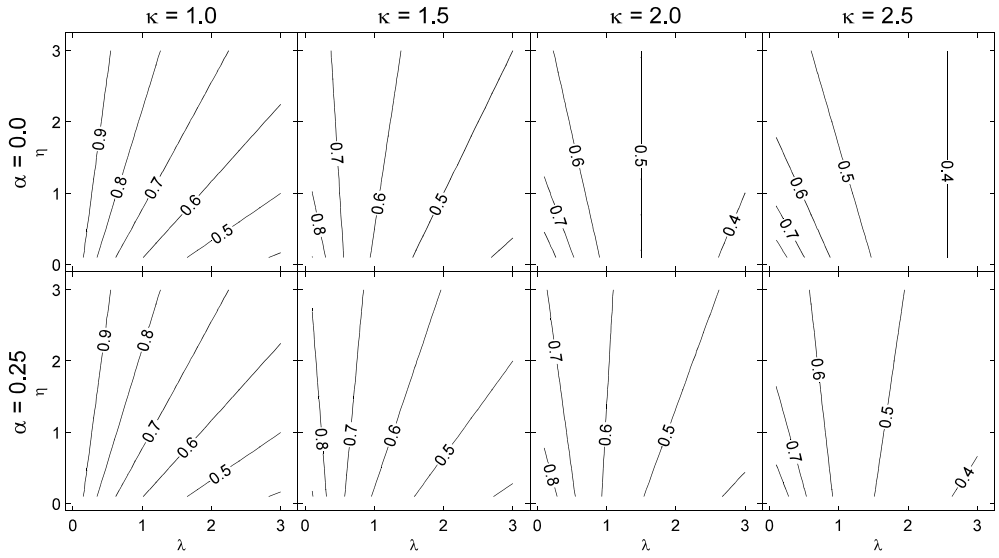

Figure 12a μ_{max}/μ_{maxs} for $\mu_{maxs} = 6$

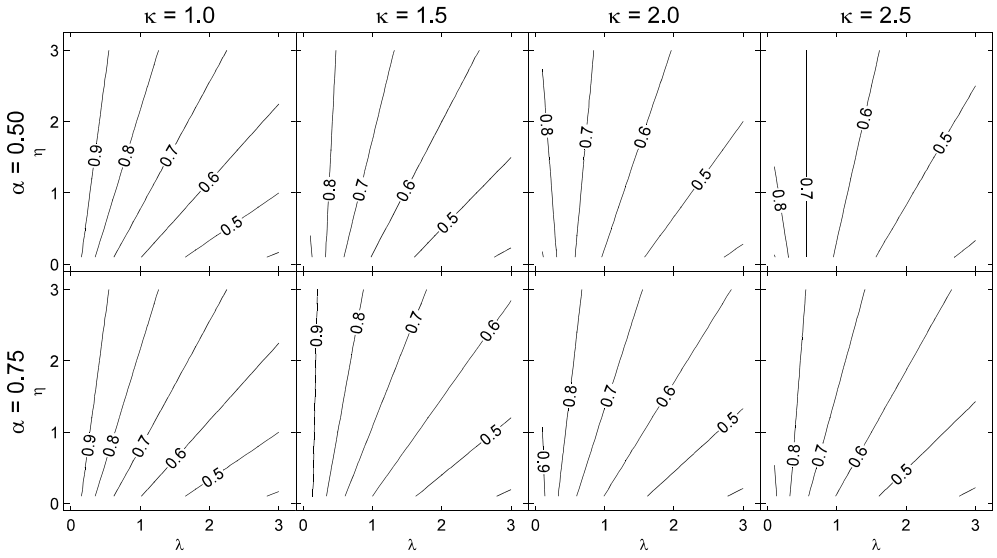

Figure 12b μ_{max}/μ_{maxs} for $\mu_{maxs} = 6$

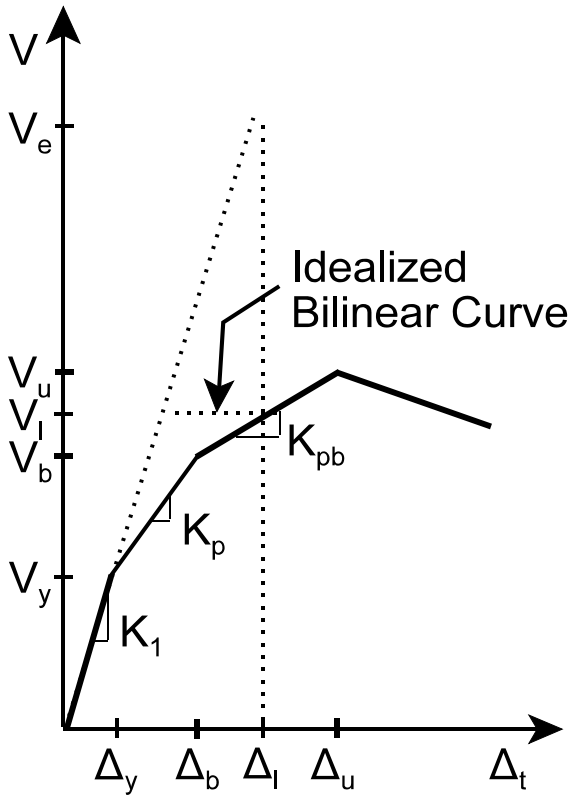

Figure 13 Retrofitted Pier Pushover Curve with Elastic Response

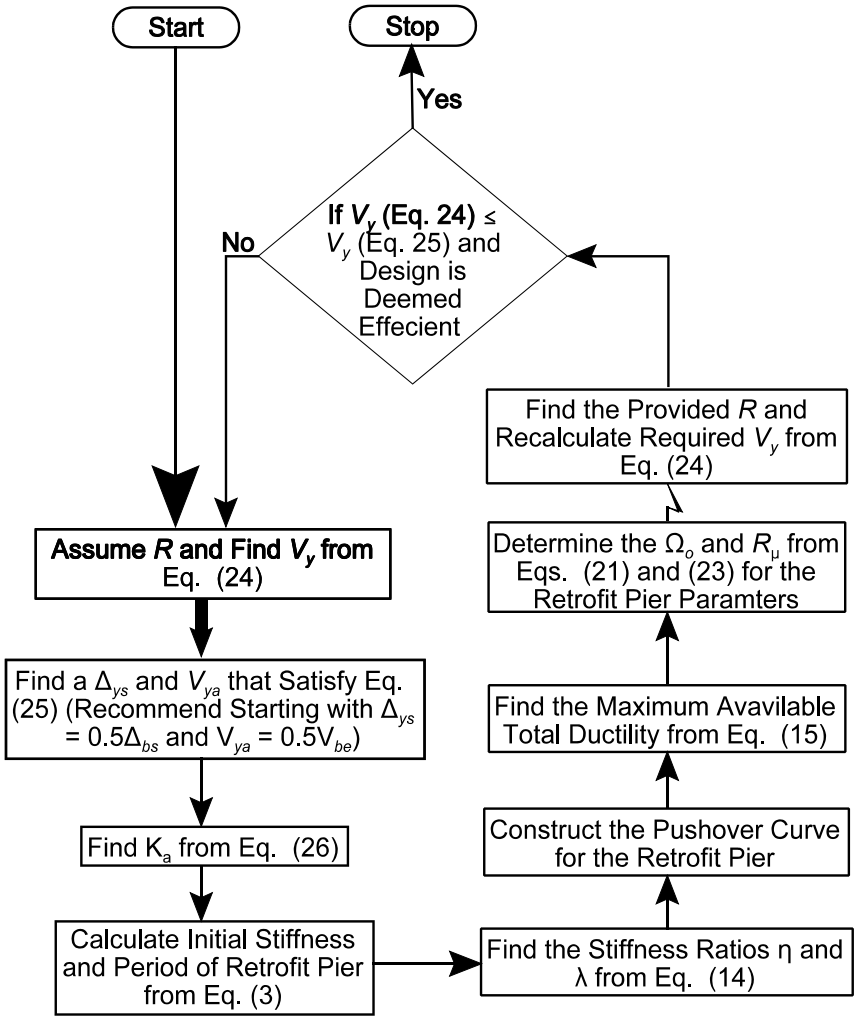

Figure 14 Flow Chart for Supplemental System Preliminary Design Procedure

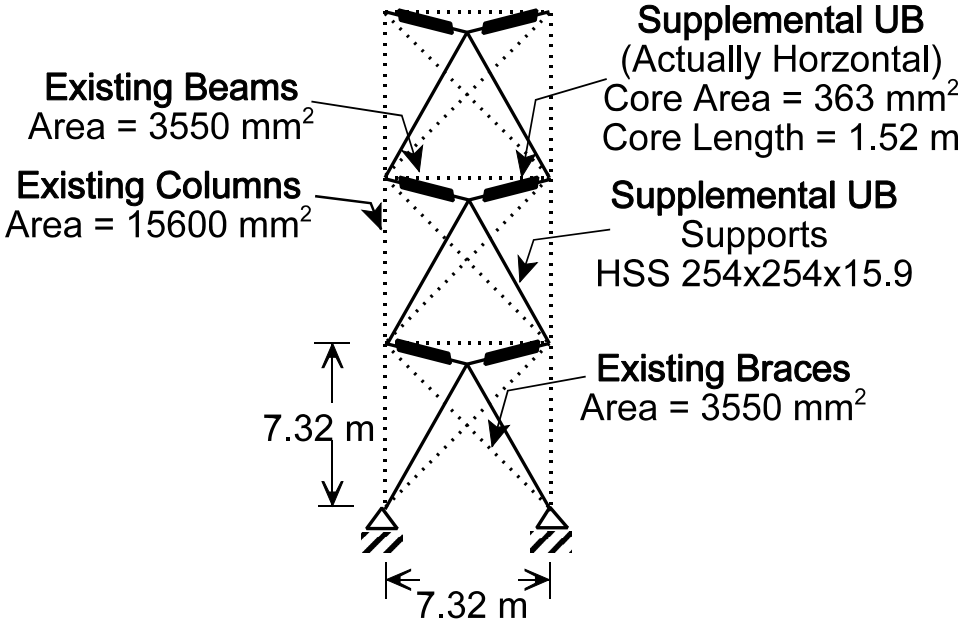

Figure 15 Schematic of Unbonded Brace (UBB) Supplemental System Retrofit Example

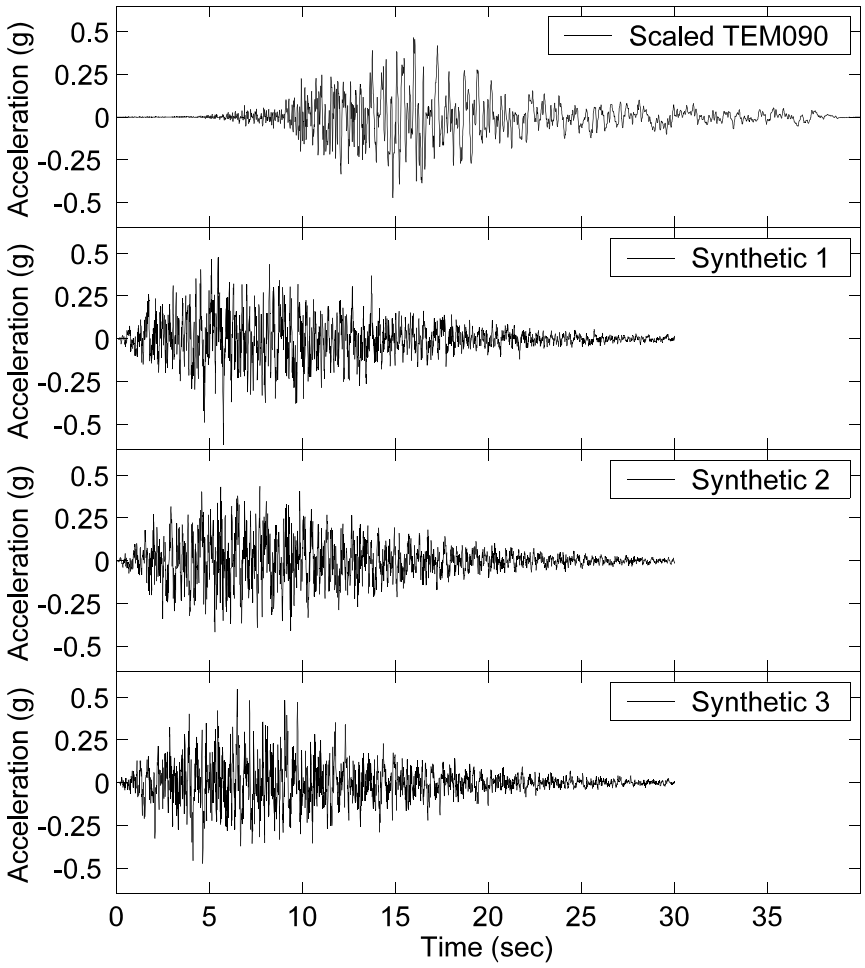

Figure 16 Acceleration Time Histories

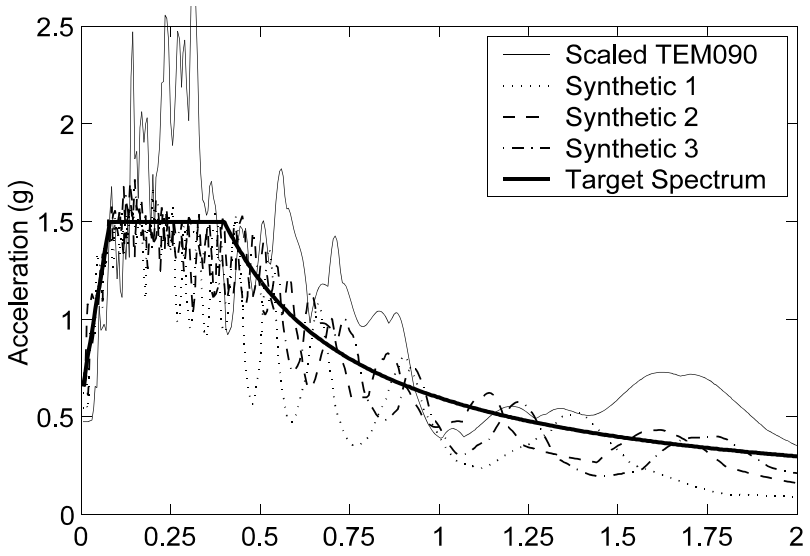

Figure 17 Acceleration Response Spectra